Asynchronous Compressive Sensing in Radar Systems

Jun Zhou[1], Samuel Palermo[1], Brian M. Sadler[2] and Sebastian Hoyos[1]

[1]Texas A&M University, College Station, TX 77843, United States
[2]Army Research Laboratory, Adelphi, MD 20783, United States

***Abstract* — In this paper we present an asynchronous compressive sensing front-end for radar systems. By using a continuous-time ternary encoding scheme (CT-TE), the amplitude variations on radar pulses are converted into timing information. The oversampling architecture mitigates the quantization error and improves time-delay estimation accuracy. The high data volume resulting from oversampling is reduced by using compressive sensing (CS) in the digital domain. Moreover, the high power consumption of randomization in an analog CS front-end is avoided in the proposed asynchronous scheme by using a part-time operation strategy in the most power demanding modules. Simulations show that the proposed scheme achieves a better range accuracy and probability of detection at sub-Nyquist rate compared to a conventional system that uses oversampling ADCs.**

***Index Terms* — asynchronous, compressive sensing, continuous-time ternary encoding, part-time randomization, time-delay accuracy.**

I. Introduction

The range resolution of a typical pulsed radar system is proportional to the bandwidth of the transmitted pulses [1], so that using high bandwidth pulses is one possibility to achieve high-resolution in radar systems. One example is linear-frequency modulated (LFM) pulse, whose bandwidth is determined by the highest chirp frequency rather than the pulse width. However, a high bandwidth pulse requires a high sampling rate that introduces significant design challenges, such as high power consumption in the high-speed analog-to-digital converter (ADC) and large volumes of data to be stored, transmitted and processed in a real-time [2].

Compressive sensing (CS) provides a way to capture some broadband signals at a sub-Nyquist rate if the signal is sparse or compressible in some domain [3]. J. Yoo, *et.al.*, applied an analog CS technique to the radar systems in [4]. However, this uses clocked PN generation with continuous-time mixing and integration, resulting in high power consumption [5]. In this paper, we present a digital-assisted asynchronous compressive sensing (DACS) front-end [6] in the radar context. By employing a continuous-time ternary encoding scheme, the pulse variations are converted into timing information. This oversampling architecture helps mitigate the quantization error generated by the low (ternary) resolution ADC. In addition, the asynchronous operation allows the analog-to-digital conversion to be free from stringent requirement on clock jitter that is a fundamental limitation for high-speed ADCs [2]. The large data volume due to oversampling is reduced by employing a digital version of the CS technique. This results in an overall sub-Nyquist sampling rate. The power consumption of the DACS front-end is also optimized by the part-time operation of power demanding modules in the asynchronous CS front-end. Simulations demonstrate that the proposed DACS front-end achieves better range accuracy and higher probability of detection at a sub-Nyquist sampling rate, as compared to a conventional system based on oversampling ADCs.

This paper is organized as follows. Section II briefly reviews the compressive sensing framework. The DACS front-end, including block diagrams of the CT-TE scheme and algorithmic logic, are introduced in Section III. Section IV presents time-delay accuracy analysis. Simulation results of the DACS front-end in a typical monostatic pulse radar system are given in Section V. Finally, Section VI concludes the paper.

II. Compressive Sensing Background

Compressive Sensing (CS) is a framework that enables sub-Nyquist sampling and processing of sparse signals. Any sufficiently sparse or compressible signal can be reliably reconstructed from a relatively small number of incoherent, randomized linear projection samples as compared to the conventional Nyquist sampling systems [3]. One unique advantage of the CS technique is that it integrates sampling and compression into one step at the analog front-end.

CS adopts a randomized sampling kernel rather than the conventional delta stream. At the digital back-end, CS recovers the original signal by solving an optimization problem,

$$\min \|x\|_0 \quad \text{subject to} \quad y = \mathbf{\Phi} x, \tag{1}$$

where $\mathbf{\Phi}$ is an $M \times N$ measurement matrix. As is well known [3], problem (1) can be relaxed to an l_1-norm problem when $\mathbf{\Phi}$ satisfies a restricted isometry property (RIP). Composing $\mathbf{\Phi}$ from Gaussian and/or symmetric Bernoulli (±1) random processes satisfies RIP with overwhelming probability [7].

III. Asynchronous Compressive Sensing Front-end

An asynchronous digital-assisted compressive sensing (DACS) front-end was presented in [6] which consists of a continuous-time ternary encoder (CT-TE) and algorithmic logic. Fig. 1 shows the CT-TE architecture. Suppose the input signal $z(t)$ has been pre-amplified to full-scale with a peak-to-peak value U. The threshold generator divides U into 2^Q levels based on quantization bit Q, and provides a threshold pair ($V_{th,L}$, $V_{th,H}$) to the comparator. The difference between $V_{th,L}$ and $V_{th,H}$ is a quantization step Δ. Visually, one threshold pair forms one comparison window, which is initialized to the input's running average. When $z(t)$ goes higher than $V_{th,H}$ or lower than $V_{th,L}$, the comparator outputs "+1" or "-1", respectively and the threshold generator updates the comparison window; otherwise, the comparator outputs "0", and the threshold pair remains unchanged. As a result, the signal variations are modulated into ternary timing information. Without loss of generality, we assign unit amplitude to the output "+1" and "-1" pulses.

Comparing with the other amplitude-to-time conversion schemes, the time encoding machine (TEM) [8], delta modulation [9], and integrate-and-fire scheme [10], the CT-TE approach has the advantage that it fires only when significant signal variation occurs. The output is ternary piecewise-constant $x(t) = \{-1, 0, 1\}$. Let us use a discrete set of times $\boldsymbol{T} = \{T_0, T_1, T_2, \ldots\}$ to represent the asynchronous time instants of each transition edge. Note that no clock is involved in the CT-TE module. The output is fully signal-driven and a function of continuous time.

In the CT-TE scheme, time periods between successive transition edges contain information. Let $T_{i\to i+1}$ denote the time period between the i^{th} and $(i+1)^{\text{th}}$ transition. $T_{i\to i+1}$ can be calculated by counting the elapsed clock cycles $C_{i\to i+1}$ of a clock that runs at a pre-defined frequency f_c,

$$T_{i\to i+1} = C_{i\to i+1}\Delta t \ , \tag{2}$$

where $\Delta t = 1/f_c$. We take f_c to be higher than the Nyquist rate of the input signal for sufficient timing resolution. For a piecewise-constant signal, we have

$$\int_{T_i}^{T_{i+1}} x(t)\cdot p_c(t)\,dt = x(t)\cdot\int_{T_i}^{T_{i+1}} p_c(t)\,dt \ , \tag{3}$$

where $p_c(t)$ stands for the chipping sequence from the PN generator. Due to the ternary characteristics, the inner product of PN sequence with zero-value sections is trivial. Hence, the PN generator is halted and all timing information of these periods can be modulated to the next nonzero-value sections, as shown in Fig. 2. In this way, an equivalent compact signal $x_{\text{eq}}(n)$ is formed for $x(n)$ as the recovery target in the l_1-norm problem. Then $x(n)$ is restored from $x_{\text{eq}}(n)$ by demodulating the zero-valued sections. The DACS front-end realizes part-time operation of PN generation and randomization, which are the most power-demanding parts in a conventional CS scheme [5]. We define the *part-time ratio* (PTR) to quantify the percentage of part-time operation,

$$r_{\text{part-time}} = \frac{\sum_{i\in x_{\text{eq}}} T_{i\to i+1}}{\sum_{i\in x} T_{i\to i+1}} \ . \tag{4}$$

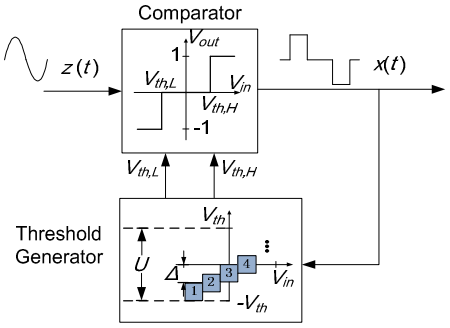

Fig. 1. Architecture of the Continuous-Time Ternary-Encoder (CT-TE).

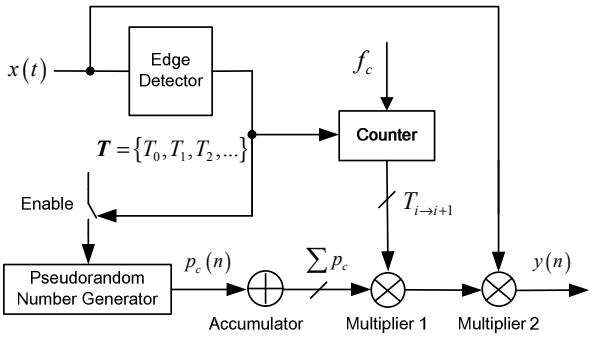

Fig. 2. Block diagram of the algorithmic logic.

IV. Time Delay Accuracy

Noise is a fundamental limitation to accurate radar measurements. There are two types of noise that are inevitable in any radar systems, thermal noise and quantization error. We consider them both in the following.

Let z denote the received baseband radar signal, which consists of a pulse reflection signal s, thermal noise n, and quantization error q. Thus we have

$$z = s + n + q \ . \tag{5}$$

In order to quantify the accuracy of the time-delay estimation, we investigate the root mean square (rms) of the difference between the estimated value and the true one. It has been shown in [1] that typical rms error in a time-delay measurement T can be expressed as

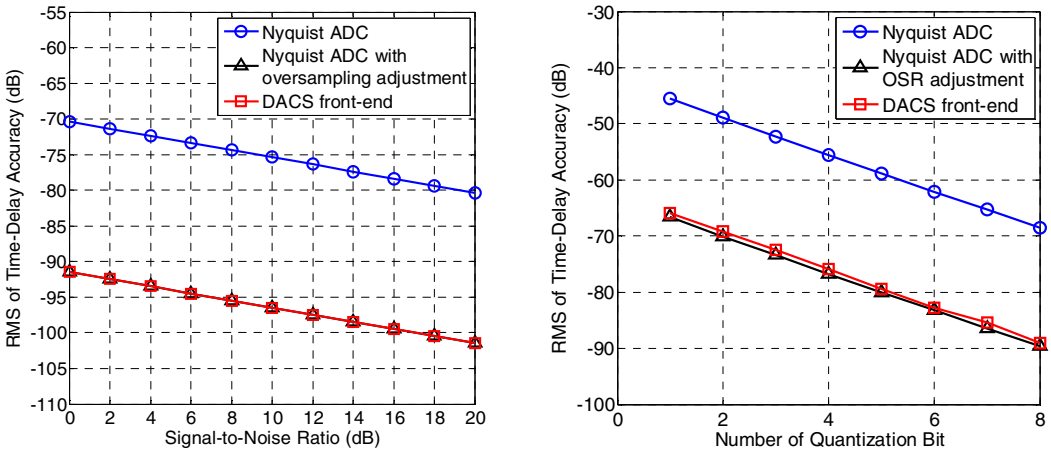

(a) (b)

Fig. 3. Quantitative effect of thermal noise and quantization noise on the rms error of time-delay measurements: (a) thermal noise is dominant; (b) quantization error is dominant.

$$T_{\text{rms}} = \frac{1}{\beta\left(2E/N_0\right)^{1/2}} \quad , \tag{6}$$

where E is the signal power, N_0 is the noise power per unit bandwidth, β is the effective bandwidth defined as

$$\beta^2 = \frac{\int_{-\infty}^{\infty}(2\pi f)^2\left|S(f)\right|^2 df}{\int_{-\infty}^{\infty}\left|S(f)\right|^2 df} \quad , \tag{7}$$

and $S(f)$ is the spectrum of pulse signal. In an ideal ADC, quantization error is uniformly distributed between $-\Delta/2$ and $+\Delta/2$. In this case, the quantization error is modeled as the white noise with a power spectrum density (PSD) of

$$\text{PSD}(q) = \frac{\Delta^2}{12 f_s} \quad . \tag{8}$$

Note that thermal noise n and quantization error q are assumed to be independent. By including both n and q, we have

$$T_{\text{rms}} = \sqrt{\frac{N_0 + Q}{2\int_{-\infty}^{\infty}(2\pi f)^2\left|S(f)\right|^2 df}} \quad . \tag{9}$$

According to (9), an accurate time delay measurement implies increasing the frequency of transmitted pulses and/or decreasing the thermal and quantization noise. Equation (8) shows that one can decrease the quantization noise by either increasing the sampling rate f_s or decreasing the quantization step Δ. Specifically, increasing the ADC resolution by 1 bit decreases the quantization noise power by 6 dB. Doubling the over-sampling rate decreases the quantization noise power by 3dB.

Fig. 3 shows the quantitative effect of thermal noise and quantization error on T_{rms}. A LFM pulse with 3MHz bandwidth and 6.7μs pulse width is simulated. Fig. 3 (a) and (b) show two cases when thermal noise and quantization noise are dominant, respectively. Two digitization schemes, a conventional Nyquist ADC and the CT-TE scheme with an oversampling ratio (OSR) of 1000, are simulated. For fair comparison, a Nyquist ADC with OSR adjustment is also provided. In Fig. 3 (a), T_{rms} for both digitization schemes decreases by 1dB when the signal-to-noise ratio (SNR) increases by 2dB. Fig. 3(b) shows that increasing one quantization bit will reduce T_{rms} by 3dB. These results are expected given equation (9).

V. Simulation

A monostatic pulsed radar system is designed to estimate target range with parameters listed in Table I. Three stationary Swerling case 2 targets are simulated, located at 2001m, 6533m and 6845m. All targets have 1m^2 radar cross section.

The DACS front-end and the conventional ADC are compared. For fair comparison, both digitization schemes are set to the same sampling rate. The performance is evaluated in terms of probability of detection (P_d) and range accuracy (A_r). The group-based total variation (GTV) algorithm [6] is used in the DACS front-end to reconstruct the equivalent compact signal $x_{\text{eq}}(n)$. To evaluate the sub-Nyquist sampling of the DACS front-end, compression ratio (CR) is taken as the ratio of the effective sampling rate of the DACS front-end to the Nyquist rate.

Fig. 4 shows the reconstruction of one reflected pulse signal. Four quantization bits and 1000 oversampling ratio are employed. The PTR of the DACS front-end is 0.00047. Combining the oversampling ratio, the CR is 0.47. The upper plot shows the transient waveform, and the bottom plot shows the relative error of the two digitization schemes. As we can see, the DACS front-end achieves better reconstruction due to the embedded Schmitt trigger in the threshold generator.

Fig. 5 shows the target detection in the DACS front-end, where the solid line is the reconstructed pulse signal. The dashed line is the power threshold for detection using Shnidman's equation. As we can see, the three targets are detected at 2003m, 6529m, and 6838m, respectively.

Monte-Carlo simulation was carried out to determine the probability of detection and range accuracy. With 4 quantization bits, the oversampled ADC achieves P_d = 99.72%, A_r = 6.4m, while the DACS front-end achieves P_d = 99.76%, A_r = 4.9m.

TABLE. I
SUMMARY OF RADAR SYSTEM PARAMETERS

Parameter	Value
Maximum unambiguous range	8km
Range resolution	50m
Transmit pulse	LFM: 3MHz bandwidth 6.67μs pulse width
Carrier frequency	10GHz
Antenna	Isotropic
Propagation environment	Two-way free space
Number of pulse for integration	10

V. CONCLUSION

In this paper, we present a digital-assisted asynchronous compressive sensing (DACS) front-end for radar systems. By using a continuous-time ternary encoding (CT-TE) scheme, the amplitude variations on radar pulses are converted into the timing information. Simulation shows that the DACS front-end achieves better range accuracy and probability of detection at sub-Nyquist rate comparing to the conventional oversampling ADC.

REFERENCES

[1] M. L. Skolnik, "Introduction to radar systems," 3rd edition, McGraw-Hill Science/Engineering/Math, Dec. 2002.

[2] B. Murmann, "Trends in low-power, digitally assisted A/D conversion," *IEICE Trans. Electron.*, vol. E93-C, no. 6, pp. 718 – 727, 2010.

[3] E. J. Candès, M. B. Wakin, "An Introduction to Compressive Sampling," *IEEE Signal Processing Magazine*, vol. 25, no. 2, Mar. 2008.

[4] J. Yoo, C. Turnes, E. B. Nakamura, C. K. Le, S. Becker, E. A. Sovero, M. B. Wakin, M. C. Grant, J. Romberg, A. Neyestanak, E. Candes, "A Compressed Sensing Parameter Extraction Platform for Radar Pulse Signal Acquistion," *IEEE Journal on Emerging and Selected Topics in Circuits and Systems*, vol. 2, no. 3, pp: 626 – 638, Sep. 2012.

[5] X. Chen, Z. Yu, S. Hoyos, B. M. Sadler and J. Silva-Martinez, "A sub-Nyquist rate sampling receiver exploiting compressive sensing," *IEEE Trans. Circuits Systems I*, vol. 58, no. 3, pp. 507-520, Mar. 2011.

[6] J. Zhou, M. Ramirez, S. Palermo, and S. Hoyos, "Digital-Assisted Asynchronous Compressive Sensing Front-end," *IEEE Journal on Emerging and Selected Topics in Circuits and Systems*, vol. 2, no. 3, pp: 482 – 492, Sep. 2012.

[7] J. A. Tropp, J. N. Laska, M. F. Duarte, J. K. Romberg and R. G. Baraniuk, "Beyond Nyquist: Efficient Sampling of Sparse Bandlimited Signals," *IEEE Trans. on Information Theory*, vol. 56, no. 1, pp. 520-544, Jan. 2010

[8] A. Lazar and L. T. Toth, "Perfect Recovery and Sensitivity Analysis of Time Encoded Bandlimited Signals," *IEEE Trans. Cir. Sys. I*, vol. 51, no. 10, pp. 2060-2073, Oct. 2004.

[9] N. S. Jayant and A. E. Rosenberg, "The preference of slope overload to granularity in the delta modulation of speech," *Bell System Technical Journal*, vol. 50, no. 10, Dec. 1971.

[10] A. S. Alvarado and J. C. Principe, "From compressive to adaptive sampling of neural and ECG recordings," in *Proc. of IEEE ICASSP,* pp. 633-636, Apr. 2011.

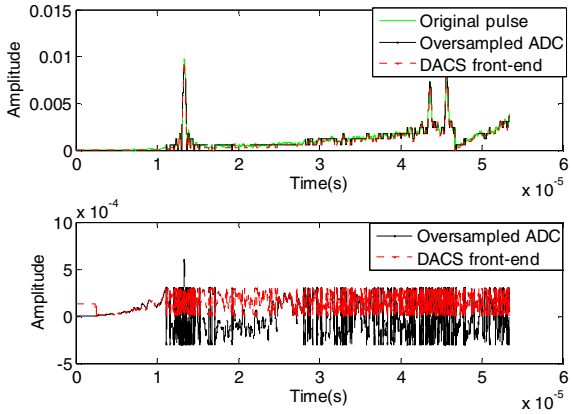

Fig. 4. Reconstruction of one reflected pulse signal: (upper plot) reconstructed waveform; (bottom plot) reconstruction error.

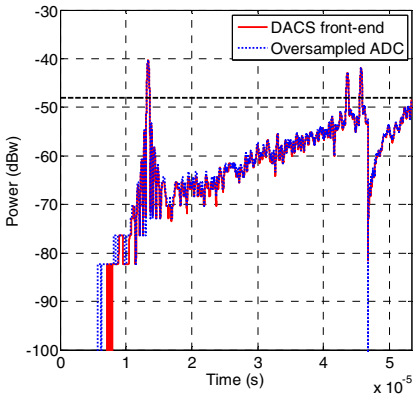

Fig. 5. Target detection using DACS front-end.